Chapter 7

High-Resolution Single-Molecule Kinesin Assays at kHz Frame Rates

Keith J. Mickolajczyk and William O. Hancock

Abstract

This chapter describes methods for high-speed, unloaded, in vitro single-molecule kinesin tracking experiments. Instructions are presented for constructing a total internal reflection dark-field microscope (TIRDFM) and labeling motors with gold nanoparticles. An AMP-PNP unlocking assay is introduced as a specialized means of capturing processive events in a reduced field of view. Finally, step-finding tools for analyzing high frame-rate tracking data are described.

Key words Kinesin, Single-molecule, Total internal reflection dark-field microscopy, Gold nanoparticle

1 Introduction

Kinesins are molecular motors that walk processively along microtubules. Advances in force-free imaging techniques have elucidated much about how kinesins hydrolyze ATP to take steps and walk in a hand-over-hand fashion [1–4]. However, the small step size and short dwell time of kinesins walking at high ATP concentrations necessitates both high spatial and temporal resolution tracking in order to measure individual steps [5–8]. Detecting the conformational changes in the motor domains that underlie the steps requires higher resolution still. New methods such as total internal reflection dark-field microscopy (TIRDFM) have been developed to meet these resolution needs [9–22], but have not yet pervaded into common use. TIRDFM offers 1 nm and 1 ms resolution, or better, and can be constructed relatively simply and inexpensively. TIRDFM works similarly to total internal reflection fluorescence microscopy (TIRF) [23, 24]. A laser light source is expanded and focused onto the back focal plane of a high numeral aperture (NA) objective. Translating the focused spot toward the periphery of the objective aperture produces light incident on the sample at an angle greater than the critical angle, resulting in total internal

Christophe Lavelle (ed.), *Molecular Motors: Methods and Protocols*, Methods in Molecular Biology, vol. 1805,
https://doi.org/10.1007/978-1-4939-8556-2_7,

reflection at the glass–water interface. In TIRDFM, the evanescent field generated from total internal reflection is used to image the positions of strongly scattering gold nanoparticles. Light scattered from gold is collected by the objective (epi configuration). Scattered light and totally internally reflected light have the same wavelength, so rather than separating them chromatically (as in TIRF), they are separated geometrically.

TIRDFM images appear very similar to TIRF images, meaning image processing and data analysis tools developed for TIRF can be directly applied to TIRDFM. The significantly stronger signal obtained from scattered light in comparison to fluorescence emission means that many more photons are collected per diffraction-limited spot per unit time, enabling higher spatial and temporal resolution tracking.

In this chapter, we first provide a walkthrough of how to construct a TIRDFM system. This relatively easy build should be achievable even in labs that do not normally focus on constructing optical systems. We next describe single-molecule assays that are optimized for high-speed imaging. Protocols include both the standard ATP landing assay and the AMP-PNP unlocking assay, which provides a way to capture motile events at very high frame rates where the exposed region of the camera is necessarily reduced [12]. By locking a kinesin with AMP-PNP and unlocking with ATP just before data acquisition [25, 26], it is possible to have a priori knowledge of where a processive run will occur rather than having to wait for rare events. The assays described here are in no way limited to TIRDFM, and are applicable to TIRF and many other imaging modalities including interferometric scattering microscopy (iSCAT), a different single-wavelength technique that has recently come into prominence as a method for very high-speed tracking of kinesin and myosin motors [9, 10, 12, 14]. To conclude, we suggest image and data analysis tools for extracting mechanistic information from movies of processive runs.

2 Materials

2.1 Buffers

1. BRB80: 80 mM PIPES, 1 mM EGTA, 1 mM $MgCl_2$, pH to 6.8 with KOH (*see* **Note 1**).
2. BRB80C: BRB80, 0.5 mg/mL casein.
3. BRB80T: BRB80, 10 μM taxol.
4. BRB80CT: BRB80, 0.5 mg/mL casein, 10 μM taxol.
5. No-nucleotide imaging solution (NN): BRB80, 0.5 mg/mL casein, 0.2 mg/mL bovine serum albumin, 10 μM taxol, 20 mM glucose, 20 μg/mL glucose oxidase, 8 μg/mL catalase, 0.5% β-mercaptoethanol (*see* **Note 2**).

2.2 Kinesins

1. Any kinesin can be used in the assays described here, and biotin-neutravidin chemistry is suggestion for motor–gold conjugation. There are many ways to biotinylate a kinesin, including Avi-tag [12], BCCP tag [27], biotin-maleimide [2, 28–30], and biotinylated antibodies [15] (*see* **Note 3**).
2. A rigor mutant of full-length kinesin-1 is suggested for immobilizing microtubules. A single point mutation (R210A in *Drosophila* KHC) will make the motor hydrolysis-incompetent and thus perfect for microtubule immobilization [12, 31].

2.3 Tubulin

1. Tubulin can be extracted from bovine brain as described in detail previously [32], or purchased from Cytoskeleton, Inc.

2.4 Molecular Probes

1. 40-nm gold nanoparticle neutravidin conjugate (Nanopartz C11-40-TN-50).
2. 150-nm gold nanoparticle neutravidin conjugate (Nanopartz C11-150-TN-50).

2.5 Flow Cells

1. Glass slides, 75 by 25 mm, thickness 1 mm (Corning 2947-75x25).
2. Rectangular glass coverslips, 24 by 30 mm, thickness 1 1/2 (Corning 2980-243).
3. Double stick tape.

2.6 Microscope

1. Optical table with passive floated legs.
2. Microscope base (Mad City Labs Micromirror TIRF system).
3. High NA objective (Olympus 60x APO N, 1.49 NA).
4. 150 mW, 532 nm CW laser (Coherent Sapphire LP) (*see* **Note 4**).
5. Basler Ace USB 3.0 CMOS camera (acA2000-165um or acA640-750um) (*see* **Note 5**).
6. Periscope assembly: Tall 1 inch post (e.g., Thorlabs RS12 and BE1), 2× counterbored post mounts (Thorlabs RM1A), 2× kinematic mounts (Thorlabs KM100), 2× 45-degree mirror mounts (Thorlabs H45), 2× broadband dielectric mirrors (Thorlabs BB1-E02).
7. Alignment tool: Slotted lens tube (Thorlabs SM1L30C), lens tube (Thorlabs SM1L20), 2× frosted glass disk with 1-mm hole (Thorlabs DG10–1500-H1), threading adapter (Thorlabs SM1A4).
8. Pinhole assembly: 25-μm pinhole (Thorlabs P25C), XY translator (Thorlabs ST1XY-A), Z-translation mount (Thorlabs SM1Z), 30 mm cage assembly rods (Thorlabs ER3-P4), 10× objective lens (L1 in Fig. 1; Thorlabs RMS10×),threading adapter (Thorlabs SM1A3) (*see* **Note 6**).

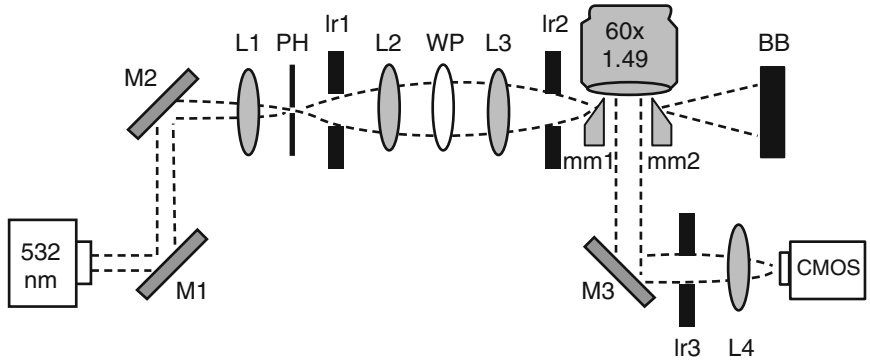

Fig. 1 Diagram of a TIRDF microscope. The beam of the table-mounted laser is first brought up to the height of the micromirrors using two mirrors (M1 and M2) in a periscope assembly. Irises Ir2 and Ir3 are used to make sure that the beam remains parallel to the optical table after the height is changed. A short focal-length lens or objective (L1) is used to clean the mode of the laser by passing it through a pinhole (PH). Light is recollimated by a second lens (L2), which has a focal length set to select a particular expansion of the beam diameter. A half-wave plate (WP) can be placed after L2 or equally anywhere in the excitation path. Lens L3 focuses the expanded laser onto the back focal plane of the high NA objective. Note that the periscope assembly could alternatively be placed between L3 and mm1. A first micromirror (mm1) is used to direct the beam onto the objective; translation of it along the optical axis will control the angle of incidence out of the objective. A second micromirror (mm2) picks the totally internally reflected beam and steers it onto a beam block (BB). Light scattered by particles in the sample is collimated by the objective and the majority of it passes in between the two mirrors. An objective coupling mirror (M3), placed at a 45 degree angle, steers the scattered light to the camera. Iris Ir3 blocks any spurious reflections. Lens L4 focuses the light onto the CMOS camera

9. Objective coupling mirror: 45 degree mirror mount (Thorlabs H45), kinematic mount (Thorlabs KM100), broadband dielectric mirror (Thorlabs BB1-E02).
10. Aspheric doublet lenses (e.g., Thorlabs AC254-XXX-A-ML) and lens holders (e.g., Thorlabs LMR1) for L2, L3, and L4. Choose L2 focal length to optimize beam expansion. Choose L3 focal length based on geometry. A shorter focal length will achieve tighter focus onto the objective back focal plane, but may generate more and closer-spaced back reflections. Choose L4 focal length to optimize magnification.
11. 3× Irises (Thorlabs ID25).
12. Base (Thorlabs CP02), lens tube (Thorlabs SM1L20) and threading adapter (Thorlabs SM1A9) for mounting Basler Ace CMOS.
13. High stability mirror mounts (Newport U100-A3K) and broadband dielectric mirrors (Thorlabs BB1-E02) for beam steering (*see* **Note 7**).
14. Miscellaneous posts, bases, and mounting forks.
15. Stage micrometer (Thorlabs R1L3S2P).
16. Half-wave plate suited for 532 nm (Thorlabs WPH05M-532).
17. Shearing interferometer (Thorlabs SI254).

3 Methods

3.1 Microscope

The optical arrangement of the TIRDF microscope is shown in Fig. 1. This setup can be achieved by customizing a TIRF inverted microscope [17], or constructed as described here (*see* **Note 8**). The custom-built design is based off the micromirror TIRF setup published by Larson et al. and Friedman et al. [33, 34], with adjustments to simplify and optimize the setup for dark field. The setup is based around a Mad City Labs RM21 microscope base, which is available together with translatable micromirrors that are placed under the high NA objective. The following protocol describes how to construct a simple custom TIRDF microscope that is ideal for single-molecule kinesin assays.

3.1.1 Excitation Line Construction

1. Secure the 532 nm laser to the optical table.
2. Secure the RM21 microscope base to the optical table, allowing enough space for excitation and emission lines to be built.
3. Set the height of the micromirrors so they sit just below the base of the objective port. Center one of the micromirrors below the objective port.
4. Make an alignment tool by placing two frosted glass alignment disks into a lens tube. Screw the alignment tool into the objective port with an appropriate threading adapter.
5. Use a periscope assembly to raise the laser height and direct it onto the micromirror. Place two irises between the periscope and the micromirror and walk the beam through them to ensure that the beam is flat. Adjust the micromirror such that the beam goes through both holes in the alignment tool.
6. Place the pinhole assembly into the optical path in front of Ir1. Adjust the position of L1 to maximize the intensity that passes through the pinhole. Adjust the position of the assembly such that the center of the diverging beam passes still through Ir1 (*see* **Note 9**).
7. Place L2 to recollimate the beam. Reposition L2 so that the beam still goes through Ir2. Use a shearing interferometer to ensure that the beam is properly collimated.
8. Place L3 approximately one focal length away from the objective. Reposition L3 such that the beam still passes through both holes of the alignment tool.
9. Remove the alignment tool and place a plain glass slide over the objective port. Look for back reflections off the glass slide, and make adjustments to the excitation path to make sure that the back reflections overlap with the incident beam.

10. Remove the glass slide and place the objective in its holder. The beam exits the objective pointed directly upward (be sure to use protective eyeware). Translate L3 along the optical path such that the diameter of the beam exiting the objective is minimized (direct it onto a distant surface like the ceiling).
11. Place a flow-cell containing 150 nm gold nanoparticles (5 pM in BRB80 buffer) on the stage. Translate the micromirror toward the edge of the objective until TIR is clearly achieved (propagation will be parallel to the coverslip). Place the second mirror to capture the TIR beam and steer it into a beam block.

3.1.2 Emission Line Construction

1. Secure the objective-coupling mirror to the optical table beneath the objective. If a sample with 150-nm gold nanoparticles is in place, the scattered light should be visible to the eye, making placement easy.
2. Place iris Ir3 after the 45 degree mirror.
3. Visually observe the intensity pattern along the emission path by blocking it with a piece of paper. If the objective is at its optimal Z position, then the scattered light will be collimated and the gold will not be visible. If the objective is not properly placed in Z, then gold nanoparticles will be visible at some point along the path. Adjust the Z position of the objective such that gold nanoparticles are not visible at any point along the emission path.
4. Place the imaging lens L4 after the iris. The focal length relative to the objective will set the magnification (*see* **Note 10**). Attempt to place the lens such that it does not displace the beam vertically or horizontally.
5. Place a piece of paper one focal length away from the imaging lens. Adjust the Z position of the objective slightly until the 150 nm gold nanoparticles become visible, if they are not already.
6. Place the CMOS camera where the piece of paper was. The gold should be clearly visible on the camera.
7. Remove the imaging lens and increase the exposure. Steer the scattered signal if necessary, so it is centered on the camera.
8. Replace the imaging lens such that the image is centered on the camera. Minimizing displacement of the beam by the imaging lens will reduce astigmatism.
9. A half-wave plate can be placed in the excitation path to adjust the polarization state. Rotate the half-wave plate to achieve the brightest PSF. This step is not strictly necessary.

3.1.3 Calibration

1. Turn the laser off, remove the 150 nm gold sample, and place a stage micrometer on the stage.

2. Transmit white light (a cell phone LED or pen light is sufficient) through the micrometer and objective. Adjust the objective Z position such that the micrometer comes into focus.
3. Take images of the micrometer, and measure the distance in pixels between the lines (in ImageJ or similar) to get a nm-to-pixel conversion. The conversion obtained should be close to the physical pixel size of the camera divided by the magnification (*see* **Note 11**).

3.1.4 Measuring and Testing the Point Spread Function

1. Place a flow cell containing 40-nm gold nanoparticles (dissolved in BRB80 or similar) on the stage and focus on particles adhered to the coverslip surface. Slightly adjust the position of the micromirror to maximize the intensity of the gold signal.
2. If there is no astigmatism, the XY point spread function (PSF) should appear as an Airy disk (Fig. 2).
3. Use the piezo Z stage to take discrete Z steps, imaging the gold at each position.
4. Observe the XZ and YZ PSFs by taking line scans through the XY PSF at each Z position (Fig. 2; *see* **Note 12**).
5. Refocus on the 40-nm gold, and take a high frame-rate movie as the piezo is stepped in X or Y in small steps (8 nm or so) separated by 500 ms dwells.
6. Fit the PSF with a 2D Gaussian (see Subheading 3.7 below) and plot the position versus time. Steps should be clearly distinguishable by eye (Fig. 2). Realign the excitation and emission paths if 8 nm steps cannot be detected.

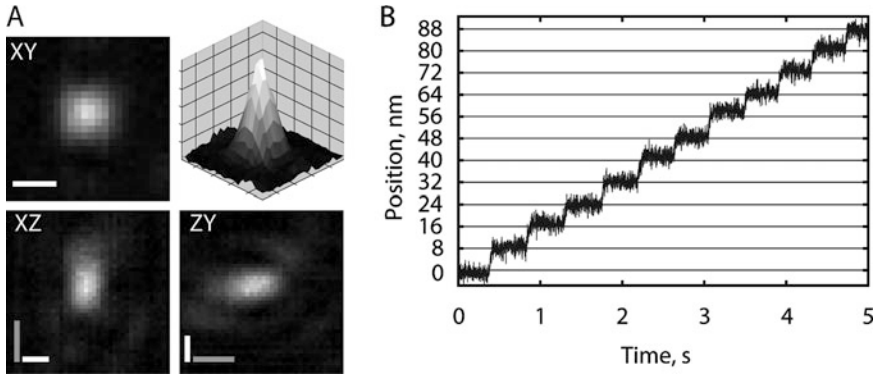

Fig. 2 Point spread functions and example steps. (**a**) Top left, an example PSF of a 40 nm gold nanoparticle in TIRDFM. This PSF should appear as an Airy disc. Scale bar is 200 nm. Top right, the same intensity information as in the top left shown as a surface plot. X and Y tick marks are 161.5 nm. Bottom, the XZ and ZY PSFs, generated by taking an X or Y line scan through the center of the XY PSF as the Z position was stepped in 50 nm intervals. These PSFs should not appear diagonal, and should appear roughly symmetrical in Z. White (X and Y) scale bars are 200 nm, and gray (Z) scale bars are 500 nm. (**b**) Example 8 nm steps with 500 ms dwells generated by stepping the piezo stage and tracking the position of an immobilized 40 nm gold nanoparticle at 1000 frames per second

3.2 Microtubule Preparation

1. Combine 10 μL of 4 mg/mL tubulin in BRB80, 1 μL 100 mM $MgCl_2$, 1 μL DMSO, 1 μL 25 mM GTP, and 10 μL BRB80 (25 μL total). Flick tube to mix.
2. Incubate at 37 °C for 30 min to polymerize.
3. Add 75 μL BRB80T to stabilize microtubules (*see* **Note 13**).
4. Dilute 10 μL of this solution into 190 μL BRB80CT (solution MT/20).

3.3 Flow Chamber Preparation

1. Wash coverslips thoroughly before use, as debris will be visible in TIRDFM. Wash first with DI water thoroughly, then incubate in 1% Hellmanex for 30 min, then wash with DI water, then wash with ethanol, and finally wash with DI water again. Blow dry (*see* **Note 14**).
2. Place two pieces of double-stick tape perpendicularly across a glass slide with about 5 mm of space between them. Trim the tape to the width of the slide with a razor blade.
3. Place the coverslip across the two pieces of tape. It is important that the length of the coverslip is greater than the width of the glass slide. A short lip of coverslip should overhang on each side of the slide, which will allow for fluid exchange after the slide is mounted upside-down on the microscope stage.
4. Fluid can be exchanged through the inverted flow cell by pipetting a drop onto one coverslip lip, and placing a small wick (i.e., a 5 cm by 1 cm piece of filter paper or paper towel) on the second lip (*see* **Note 15**).

3.4 Microtubule Immobilization for Single-Molecule Assays

1. Create a flow chamber and flow through 20 μL BRB80C. Wait 5 min. Casein will block the surface for proper binding of the rigor mutant tails to the glass surface [35, 36].
2. Dilute rigor mutant to 200 nM in casein solution plus 1 μM ATP. Add 20 μL to the flow cell and wait 5 min (*see* **Note 16**).
3. Remove excess rigor mutants from the flow cell by flushing through 20 μL casein solution.
4. Add 20 μL MT/20 solution to flow cell. Wait 5 min.
5. Remove excess microtubules from the flow cell by flushing through with 20 μL NN solution
6. Microtubules can be visualized in TIRDFM if the electric field vector of incident light is perpendicular to their long axes (Fig. 3; *see* **Note 17**). Ensure proper immobilization by inspecting for persistent, weak, time-varying signals near the surface (*see* **Note 18**). Alternatively, fluorescent microtubules can be visualized in TIRF simply by placing an emission filter in the emission path (Fig. 3). Note that the rigor mutants in the flow cell should not be left without nucleotide for long periods of time.

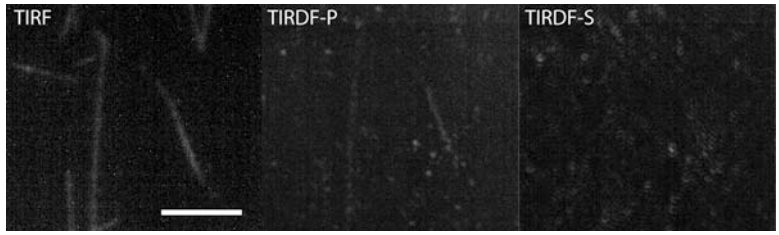

Fig. 3 Microtubule visualization. Left, rhodamine-labeled microtubules are visualized in TIRF by placing a 565 nm long-pass filter in the emission path. All fluorescent microtubules are visible at a 200 ms exposure time. Center, only vertically aligned microtubules are visible when the emission filter is removed and exposure time is reduced to 20 ms, as the linear polarization state of incident light has its electric field vector aligned perpendicular to them [23]. Right, switching linear polarizations by rotating the half wave plate results in no microtubules being visible (same 20 ms exposure). If the flow cell were rotated 90 degrees, different microtubules would be visible or invisible

3.5 Single-Molecule Landing Assay

1. Dilute Avi-tagged kinesin motor and neutravidin-gold nanoparticles to 100 pM of each in NN solution plus the desired ATP concentration (*see* **Note 19**).
2. Invert the tube to ensure that nanoparticles go into solution. Let mix on ice for at least 30 min.
3. Create a flow cell and immobilize microtubules on the surface as in Subheadings 3.3 and 3.4.
4. Flow in 20 μL NN solution plus the desired ATP concentration (*see* **Note 20**).
5. Flow in 20 μL of the motor–gold solution prepared in **step 1**. Landing events should begin occurring immediately and processive runs should be evident.
6. Adjust the Z position of the stage to optimize the signal obtained from moving particles. This focal plane may differ from the position that optimizes signal from particles nonspecifically bound to the surface.
7. Adjust the position of the micromirror to optimize the apparent signal-to-noise ratio if freely diffusing nanoparticles give too large of a background signal. Moving the mirror closer to the periphery of the objective will increase the angle of incidence and thus the initial intensity and penetration depth of the evanescent field [23].
8. Adjust the exposure time, frame rate, and exposed chip size of the camera as desired.
9. Begin taking movies. Be sure to test the analysis scheme before building large data sets (*see* **Note 21**).

3.6 Single-Molecule AMP-PNP Unlocking Assay

1. Dilute Avi-tagged kinesin motor and neutravidin-gold nanoparticles to 100 pM of each in NN solution plus 1 mM AMP-PNP.

2. Invert the tube to ensure that nanoparticles go into solution. Let mix on ice for at least 30 min.
3. Create a flow cell and immobilize microtubules on the surface as in Subheadings 3.3 and 3.4.
4. Flow in 20 μL NN solution plus 1 mM AMP-PNP (*see* **Note 22**).
5. Flow in 20 μL of the motor–gold solution prepared in **step 1**. Landing events should begin occurring immediately, but no particles should move after landing.
6. Allow 3–5 min for AMP-PNP-locked motors to accumulate on the microtubules.
7. Adjust the Z position of the stage and the micromirror position to optimize the signal from locked motor–gold complexes (*see* **Note 23**).
8. Adjust the position of the micromirror to optimize the total signal from a locked motor–gold complex. The bulk will be cleared before image acquisition, which minimizes the free nanoparticle background signal. Thus, the strongest possible evanescent wave should be used.
9. Adjust the exposure time, frame rate, and exposed chip size of the CMOS as desired. Center one or more locked motor–gold complexes on screen (*see* **Note 24**).
10. Taking great care not to jostle the flow cell, flow in 40 μL NN solution plus 2 mM ATP (*see* **Note 25**).
11. Fluid exchange will make the flow cell swell, and thus the sample will fall out of focus. Readjust the Z position of the stage as needed.
12. As soon as the chamber is cleared, motors will begin to unlock following an exponential distribution with a mean of approximately 30 s. Begin taking movies one after another as soon as **step 11** is complete.
13. Once all molecules are unlocked, the assay is over. Refill the chamber by going back to **step 4** and repeating. It is not recommended to refill a chamber more than 3 times due to accumulation of dead motors and nonspecifically bound gold.
14. Make new flow cells and repeat as desired.

3.7 Image Analysis

The PSF apparent in TIRDFM is very similar to TIRF, and will be an Airy Disk if setup properly. Thus, the many well-developed tools for subdiffraction limited particle tracking in fluorescence imaging (such as FIONA) can be used for TIRDFM images [2, 37]. These tools generally work by estimating the central order of the Airy Disk as a 2D Gaussian function, and performing nonlinear regression to find the Gaussian parameters that minimize residuals with the pixel

intensity values of the PSF. The parameters returned will include nanometric estimations of X and Y position over time, as well as errors on the estimations (*see* **Note 26**). A very useful free Gaussian fitting software is FIESTA, released by B CUBE Center for Molecular Bioengineering at Technische Universitaet Dresden [38].

3.8 Step-Finding and Data Analysis

In order to extract steps from the time versus position (X, Y, t) traces obtained from the image analysis software, a step-finding algorithm is applied. The analysis performed depends on the design of the experiment and the parameters one wishes to determine, but in all cases it is best to try both a model-free and model-dependent step-finding algorithm. A model-free step-finding algorithm places steps based solely on statistically significant differences within the data, with no knowledge or assumption on what the step size is or how many steps are expected. Our lab has recently released free versions of two model-free algorithms, tDetector and bDetector, which have been applied to kinesins stepping as well as photobleaching data [12, 39]. A model-dependent step-finding algorithm uses prior knowledge, such as the microtubule lattice spacing [12] or the approximate number of steps [40], in order to fit steps. Model-free algorithms will often overfit the data, making measurements such as dwell times difficult. Model-dependent algorithms overcome this difficulty, but it is essential to justify their use by first proving their basis with a model-free algorithm.

4 Notes

1. The ionic strength of BRB80 buffer is near physiological ionic strength and is highly recommended. Reducing the ionic strength can enhance motor–microtubule interactions, which can make data collection easier, but it results in nonspecific motor–microtubule interactions that can mask measurement the true kinesin mechanochemistry [41, 42].
2. Nucleotides (ATP or AMP-PNP in this protocol) should be prepared with equimolar $MgCl_2$. Magnesium is necessary for proper kinesin function [43].
3. Our lab has adopted Avi-tagging as the primary means of biotinylation, as cysteine-light versions of kinesin-1 have been seen to exhibit different force-velocity behavior than wild-type [44]. Whatever biotinylation and molecular probe strategy is chosen, it is important to run control experiments to make sure that the tagging scheme does not alter velocity and run length.
4. This wavelength of 532 nm is set to match the surface plasmon of 40-nm gold nanoparticles, and so will produce a strong scattering signal for that probe. The scattering amplitude

depends strongly on the incident wavelength, with lower wavelengths producing stronger signals. Longer wavelengths are, however, gentler on the sample. It is recommended to match the wavelength to the surface plasmon resonance peak of the nanoparticle primarily used.

5. The Basler Ace CMOS is a great camera choice since it is inexpensive, small, has suitable quantum efficiency and gain, can achieve moderate high frame rates, and utilizes USB 3.0 connection so can be used with almost any computer. It also comes with free imaging software and LabVIEW drivers. Many other CMOS and CCD cameras also work well for TIRDFM. A Camera-Link connection will in almost all cases allow for higher frame rates, but requires additional hardware. Unlike single-molecule TIRF, an expensive camera is not strictly necessary in TIRDFM.
6. The pinhole assembly is used as part of a spatial filter, which will clean the mode of the laser. This is very important for success in TIRDFM, and has been found to be helpful even with single-mode lasers. An alternative to the spatial filter is a single-mode optical fiber. This may be more convenient than a periscope and spatial filter, but will result in more laser power loss.
7. The minimal setup described here does not include additional mirrors. However, placement of mirrors allows for greater beam control and a more compact optical setup. Placement of two mirrors in series allows for one to walk the beam through two irises, as is suggested here using the two mirrors in the periscope.
8. As shown in Fig. 1, the excitation beam is converging when it falls incident on the 45 degree mirror. Thus, the closer the 45 degree mirror is to the back focal plane of the objective, the smaller it can be. In the Ueno et al. design [17], the perforated mirror is placed in a filter cube and thus is a set distance away from the base of the objective. This distance cannot readily be controlled, and is longer than desirable, thus inherently limiting the size of the "hole" through which scattered light is captured, and reducing the NA of the setup.
9. It is critical to mount the pinhole assembly as stably as possible. Two one-inch diameter posts are recommended.
10. Total magnification will equal the objective magnification times the imaging lens focal length divided by the manufacturer-expected tube lens focal length (180 mm for Olympus). For example, a 500 mm lens after the 60× Olympus objective will give 167× magnification. A 1000 mm lens would give 333× magnification. The magnification should be set such that the conversion factor will be in the range of 30–70 nm/pixel for single-molecule tracking.

11. For example, the Basler Ace has a physical pixel size of 5.5 microns. Thus, with 167× magnification, it should be expected to achieve roughly 33 nm/pixel. The measured value will be close to, but not exactly the same as, the calculated value, and should be trusted as the true calibration.
12. If there is astigmatism or if the excitation beam is incident on the back aperture of the objective at an angle, then the XY PSF will appear oblong, and the XZ and YZ PSF will appear diagonal and asymmetrical.
13. For fluorescent microtubules, it is highly recommended to centrifuge down the product at this step (using Airfuge or equivalent), and to discard the supernatant and rinse the pellet in BRB80T. This procedure removes excess free dye and unpolymerized tubulin [32]. For unlabelled microtubules, pelleting is not necessary.
14. Dust, debris, and indeed anything that can scatter will be visible in TIRDFM, and can distract from or confound the desired signal. Thus, thorough washing is absolutely necessary.
15. Using a small wick with crisp corners is highly recommended, since it can be gently placed onto the lip of the flow chamber to absorb fluid without applying any force that may move the coverslip. This is critical for not jostling the flow cell in the AMP-PNP unlocking assay.
16. Once immobilized in the flow chamber, the rigor mutants will have their motor domains free to tightly bind microtubules. However, they may release the microtubules if, at any point, there is not at least 1 μM $MgCl_2$ present in the flow cell. This condition can lead to very slow microtubule gliding that complicates the experiments. Also noteworthy, if the kinesin being tested also has the full length kinesin-1 tail, then it too can bind to the casein-treated glass surface and may lead to gliding.
17. Microtubules will be visible in TIRDFM if the electric field vector is perpendicular to their long axis. This can be taken advantage of in order to visualize the microtubules, but should be minimized when imaging gold nanoparticles. Control the geometry of the flow cell (microtubules tend to align in flow) and the polarization state of the incident light (using the half-wave plate) to manage this.
18. In our experience, the largest problem limiting spatial resolution in kinesin tracking assays is lack of complete microtubule immobilization on the surface. Other immobilization methods, such as anti-tubulin antibodies, have been found to be insufficient in our hands, and rigor mutants have been the best solution. If microtubules wobble even with the rigor immobilization, making a new preparation of rigor mutant protein is recommended.

19. It is important to ensure that only one active kinesin binds to each gold nanoparticle. The equimolar 100 pM working concentration is recommended, but the necessary amount of motor might change depending on the relative activity and degree of biotinylation of the motor preparation. It is highly recommended to carry out control assays to identify an optimal working concentration by maintaining the gold concentration at 100 pM and varying the motor dimer concentration. Count the number of landing events that occur per second per micron of microtubule. In order to best count the microtubules, it may be easiest to use fluorescently labeled microtubules and insert a long-pass emission filter right before the camera (switching to TIRFM). According to Poisson statistics, if the number of landing events increases linearly with the motor concentration, then there is only one motor per gold nanoparticle [35]. At motor concentrations where more than one motor binds to each gold nanoparticle, the landing rate versus motor concentration curve will begin to plateau [45]. Choose a working concentration from the linear regime.
20. Each exchange through the flow cell may only actually remove about 80% of the fluid. Thus, to tightly control the ATP concentration, it is recommended to already have the desired ATP concentration in the flow cell before exchanging fluids to add motors.
21. It is recommended to take movies from multiple flow cells on multiple days when building up a data set. This approach averages out the effects of any errors inherent to a given preparation or flow cell. Additionally, temperature can be a significant factor in single-molecule assays [46]. Illuminating a sample with laser light will heat it up over time. Significant velocity increases will occur if the sample heats up. A single flow cell should not stay on the microscope for more than 20 min. It is highly recommended to keep a thermometer on the microscope base and make sure that all measurements are done at the same console temperature.
22. Be sure to make the AMP-PNP stocks with equimolar $MgCl_2$.
23. Even with good surface blocking, some degree of nonspecific binding is inevitable. Motor–gold complexes on the microtubule can be differentiated because they will colocalize with microtubules, or will appear "lined up" if the microtubules are not visible.
24. Exposing only a small portion of the CMOS chip will allow for much higher frame rates. However, it will make landing assays extremely difficult. Once a few coaligned AMP-PNP locked motors are found, the field of view can be shrunk down to a tiny size with the locked motors centered in it. Thus, events can easily be measured even with the tiny field of view.

25. A strategy for not jostling the flow cell is as follows. Place the 40 μL in a single drop on one lip of the flow cell. After a few seconds, the liquid line on the opposite lip will reach the edge of the coverslip. Gently drop a wick at the opposite lip, and flow through will begin to occur. Start refocusing the stage as soon as the wick is dropped.
26. The error on the X and Y localization determined by the fitting software will usually be only 1–2 nm. This does not, however, mean that one truly has a 1–2 nm positional baseline in kinesin tracking assays. Additional noise will be introduced by any wobbling of the microtubule immobilization system, stage drift, the compliance of the motor–gold linkage, and spurious signals like unbound gold nanoparticles diffusing into the area of the walking motor.

References

1. Hackney DD (1994) Evidence for alternating head catalysis by kinesin during microtubule-stimulated ATP hydrolysis. Proc Natl Acad Sci U S A 91(15):6865–6869
2. Yildiz A, Tomishige M, Vale RD (2004) Kinesin walks hand-over-hand. Science 303:676–678
3. Hancock WO, Howard J (1999) Kinesin's processivity results from mechanical and chemical coordination between the ATP hydrolysis cycles of the two motor domains. Proc Natl Acad Sci U S A 96(23):13147–13152
4. Coy DL, Wagenbach M, Howard J (1999) Kinesin takes one 8-nm step for each ATP that it hydrolyzes. J Biol Chem 274 (6):3667–3671
5. Schnitzer MJ, Block SM (1997) Kinesin hydrolyses one ATP per 8-nm step. Nature 388 (6640):386–390
6. Block SM (2007) Kinesin motor mechanics: binding, stepping, tracking, gating, and limping. Biophys J 92(9):2986–2995
7. Carter NJ, Cross RA (2005) Mechanics of the kinesin step. Nature 435(7040):308–312
8. Toprak E, Yildiz A, Tonks M, Rosenfeld SS, Selvin PR (2009) Why kinesin is so processive. Proc Natl Acad Sci U S A 106 (31):12717–12722
9. Andrecka J et al (2015) Structural dynamics of myosin 5 during processive motion revealed by interferometric scattering microscopy. elife 4: e05413
10. Ortega Arroyo J et al (2014) Label-free, all-optical detection, imaging, and tracking of a single protein. Nano Lett 14:2065–2070
11. Dunn AR, Chuan P, Bryant Z, Spudich JA (2010) Contribution of the myosin VI tail domain to processive stepping and intramolecular tension sensing. Proc Natl Acad Sci U S A 107(17):7746–7750
12. Mickolajczyk KJ, Deffenbaugh NC, Ortega Arroyo J, Andrecka J, Kukura P, Hancock WO (2015) Kinetics of nucleotide-dependent structural transitions in the kinesin-1 hydrolysis cycle. Proc Natl Acad Sci U S A 112(52): E7186–E7193
13. Nan X, Sims PA, Xie XS (2008) Organelle tracking in a living cell with microsecond time resolution and nanometer spatial precision. ChemPhysChem 9(5):707–712
14. Ortega-Arroyo J, Kukura P (2012) Interferometric scattering microscopy (iSCAT): new frontiers in ultrafast and ultrasensitive optical microscopy. Phys Chem Chem Phys 14 (45):15625–15636
15. Schneider R, Glaser T, Berndt M, Diez S (2013) Using a quartz paraboloid for versatile wide- field TIR microscopy with sub-nanometer localization accuracy. Opt Express 21(3):686–689
16. Sowa Y, Steel BC, Berry RM (2010) A simple backscattering microscope for fast tracking of biological molecules. Rev Sci Instrum 81 (11):113704
17. Ueno H et al (2010) Simple dark-field microscopy with nanometer spatial precision and microsecond temporal resolution. Biophys J 98(9):2014–2023
18. Dunn AR, Spudich JA (2007) Dynamics of the unbound head during myosin V processive

translocation. Nat Struct Mol Biol 14 (3):246–248

19. Braslavsky I et al (2001) Objective-type dark-field illumination for scattering from microbeads. Appl Opt 40(31):5650–5657
20. Yasuda R, Noji H, Yoshida M, Kinosita K, Itoh H (2001) Resolution of distinct rotational substeps by submillisecond kinetic analysis of F1-ATPase. Nature 410(6831):898–904
21. Chen G-Y, Mickolajczyk KJ, Hancock WO (2016) The kinesin-5 chemomechanical cycle is dominated by a two-heads-bound state. J Biol Chem 291(39):20283–20294
22. Mickolajczyk KJ, Hancock WO (2017) Kinesin processivity is determined by a kinetic race from a vulnerable one-head-bound state. Biophys J 112(12):2615–2623
23. Axelrod D, Burghardt TP, Thompson NL (1984) Total internal reflection fluorescence. Annu Rev Biophys Bioeng 13:247–268
24. Tokunaga M, Kitamura K, Saito K, Iwane a H, Yanagida T (1997) Single molecule imaging of fluorophores and enzymatic reactions achieved by objective-type total internal reflection fluorescence microscopy. Biochem Biophys Res Commun 235(1):47–53
25. Chen G-Y, Arginteanu DFJ, Hancock WO (2015) Processivity of the kinesin-2 KIF3A results from rear head gating and not front head gating. J Biol Chem 290 (16):10274–10294
26. Schnapp BJ, Crise B, Sheetz MP, Reese TS, Khan S (1990) Delayed start-up of kinesin-driven microtubule gliding following inhibition by adenosine 5′-[beta,gamma-imido]triphosphate. Proc Natl Acad Sci U S A 87 (24):10053–10057
27. Berliner E, Young EC, Anderson K, Mahtani HK, Gelles J (1995) Failure of a single-headed kinesin to track parallel to microtubule protofilaments. Nature 373:718–721
28. Guydosh NR, Block SM (2009) Direct observation of the binding state of the kinesin head to the microtubule. Nature 461 (7260):125–128
29. Mori T, Vale RD, Tomishige M (2007) How kinesin waits between steps. Nature 450 (7170):750–754
30. Verbrugge S, Lansky Z, Peterman EJG (2009) Kinesin' s step dissected with single-motor FRET. Proc Natl Acad Sci U S A 106 (42):17741–17746
31. Farrell CM, Mackey AT, Klumpp LM, Gilbert SP (2002) The role of ATP hydrolysis for kinesin processivity. J Biol Chem 277 (19):17079–17087
32. Uppalapati M, Huang Y, Shastry S, Jackson TN, Hancock WO (2009) Microtubule motors in microfluidics. Methods in bioengineering: microfabrication and microfluidics, pp 311–337
33. Larson J et al (2014) Design and construction of a multiwavelength, micromirror total internal reflectance fluorescence microscope. Nat Protoc 9(10):2317–2328
34. Friedman LJ, Chung J, Gelles J (2006) Viewing dynamic assembly of molecular complexes by multi-wavelength single-molecule fluorescence. Biophys J 91(3):1023–1031
35. Block SM, Goldstein LS, Schnapp BJ (1990) Bead movement by single kinesin molecules studied with optical tweezers. Nature 348 (6299):348–352
36. Ozeki T et al (2009) Surface-bound casein modulates the adsorption and activity of kinesin on SiO2 surfaces. Biophys J 96 (8):3305–3318
37. Yildiz A (2003) Myosin V walks hand-over-hand: single fluorophore imaging with 1.5-nm localization. Science 300 (5628):2061–2065
38. Ruhnow F, Zwicker D, Diez S (2011) Tracking single particles and elongated filaments with nanometer precision. Biophys J 100 (11):2820–2828
39. Chen Y, Deffenbaugh NC, Anderson CT, Hancock WO (2014) Molecular counting by photobleaching in protein complexes with many subunits: best practices and application to the cellulose synthesis complex. Mol Biol Cell 25(22):3630–3642
40. Kerssemakers JWJ et al (2006) Assembly dynamics of microtubules at molecular resolution. Nature 442(7103):709–712
41. Shastry S, Hancock WO (2010) Neck linker length determines the degree of processivity in kinesin-1 and kinesin-2 motors. Curr Biol 20(10):939–943
42. Shastry S, Hancock WO (2011) Interhead tension determines processivity across diverse N-terminal kinesins. Proc Natl Acad Sci U S A 108(39):16253–162588
43. Cohn SA, Ingold AL, Scholey JM (1989) Quantitative analysis of sea urchin egg kinesin-driven microtubule motility. J Biol Chem 264(8):4290–4297
44. Andreasson JO et al (2015) Examining kinesin processivity within a general gating framework. elife 4:e07403
45. Hancock WO, Howard J (1998) Processivity of the motor mrotein kinesin requires two heads. J Cell Biol 140(6):1395–1405
46. Nara I, Ishiwata S (2006) Processivity of kinesin motility is enhanced on increasing temperature. Biophysics (Oxf) 2:13–21